

AEC008

Numerical Analysis of Syngas non-premixed Combustion in a Round-Jet Porous Burner

Santiphong Klayborworn¹ and Watit Pakdee^{1,*}

¹ Department of Mechanical Engineering, Thammasat University, Klong Luang, Pathumthani, 12120 Thailand

* Corresponding Author: E-mail: pwatit@engr.tu.ac.th, Phone: 02 564-3001 to 9 ext 3143, Fax: 02 564-3023

Abstract

This paper presents the simulations of non-premixed turbulent combustion of syngas (synthesis gas) in a round-jet porous burner. Syngas is a gas mixture, primarily composed of hydrogen, carbon monoxide and carbon dioxide. The name syngas relates to its use in creating synthetic natural gas. In the model, syngas is fed from a pipe into a porous region with a slow co-flow of air. Upon exiting the pipe, the syngas mixes and combusts with the surrounding air in a non-premixed manner. The resulting turbulent flame is attached to the burner head. The model is solved by combining the Reacting Flow and the Heat Transfer in Fluids interfaces. The turbulent flow in the jet is modeled using the $k - \omega$ turbulence model, and the turbulent reactions are modeled using the eddy dissipation model. The resulting computed velocity, temperature and species mass fractions in the reacting jet are investigated.

Keywords: non-premixed, turbulent combustion, round-jet porous burner, syngas

1. Introduction

The name syngas gives reference to the role of this fuel gas mixture comprised mostly of hydrogen, carbon monoxide, and carbon dioxide as an intermediate in the production process of synthetic natural gas. Syngas, however, is also used to create other products such as methanol, ammonia, and even hydrogen. Unlike direct coal combustion, hydrogen combustion produces virtually no pollution or greenhouse gases while syngas produces much less emissions. Therefore ongoing development of hydrogen and syngas combustion technology as an appropriate type of future energy source is playing an increasingly important role in the clean energy strategy. Particularly there is a growing interest in the combustion of hydrogen-enriched synthesis gas. H₂/CO syngas non-premixed impinging jet flames were studied using three-dimensional direct numerical simulation (DNS) and flamelet generated manifolds (FGM) based on detailed chemical kinetics [1]. Results showed that the ratio of H₂ and CO in the syngas mixture significantly affects the flame characteristics including the near-wall flame structure. This model simulates turbulent combustion of syngas (synthesis gas) in a simple round jet burner. Syngas is a gas mixture, primarily composed of hydrogen, carbon monoxide and carbon dioxide. The name syngas relates to its use in creating synthetic natural gas. The non-premixed combustion of CO/H₂ mixtures in a round-jet burner was numerically studied by Cauci et al [2]. The temperature and composition resulting from the non-premixed CO/H₂/N₂ combustion in the round-jet burner have also been experimentally investigated by Barlow and co-workers [3-4] as a part of the International Workshop on Measurement and Computation of Turbulent Nonpremixed Flames [5]. The model is solved in COMSOL Multiphysics by combining a Reacting Flow and a Heat Transfer in Fluids interface. The previous work on modeling the

non-premixed combustion in a porous burner is very limited. The numerical simulation of methane/air non-premixed combustion in porous media was investigated [6]. The results showed that combustion efficiency was improved in porous media with significantly lower NO_x and CO emissions. In the present study, we study the non-premixed turbulent combustion using syngas in a round-jet porous burner.

2. Model Definition

In the present study, the porous medium is assumed to be in local thermal equilibrium (LTE). Such a model can be used if the mass flow density, pore diameter, and porosity are not too high and if the heat transport properties and the temperature are not too low [7]. This model was successfully employed in the investigation of methane-air non-premixed combustion in porous media [8]. The numerical calculations were consistent with experiment data. Further, the same LTE was used to numerically investigate porous combustion for HCl synthesis [9] wherein the adiabatic flame temperature and flame speed were successfully carried out.

The porous burner studied in this model consists of a straight pipe placed in a slight co-flow. The gas phase fuel is fed through the pipe using an inlet velocity of 76 m/s, while the co-flow velocity outside of pipe is 0.7 m/s. Schematic representation of the problem is depicted in Figure 1.

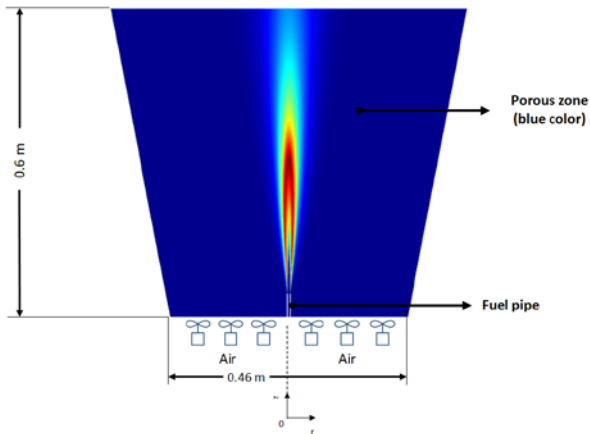


Figure 1: Schematic representation of the physical problem

At the pipe exit, the fuel gas mixes with the co-flow, creating a circular jet confined in a porous domain. The gas fed through the tube consists of three compounds typical of syngas; carbon monoxide (CO), hydrogen (H₂) and nitrogen (N₂). The co-flow gas consists of air. At the pipe exit, the fuel is ignited. Since the fuel and oxidizer enter the reaction zone separately, the resulting combustion is of the non-premixed type. A continuous reaction requires that the reactants and the oxidizer are mixed to stoichiometric conditions. In this set-up the turbulent flow of the jet will effectively mix the fuel from the pipe with the co-flowing oxygen. Furthermore the mixture needs to be continuously ignited. In this burner the small recirculation zones generated by the pipe wall thickness provide the means to decelerate hot product gas. The recirculation zones hereby promote continuous ignition of the oncoming mixture and stabilizes the flame at the pipe orifice. In the experiments [5] no lift-off or localized extinction of the flame has been observed.

In the current study, the syngas combustion is modeled using two irreversible reactions:



This assumption of a complete oxidation of the fuel corresponds to one of the approaches used in [2]. The mass transport in the reacting jet is modeled by solving for the mass fractions of six species; the five species participating in the reactions and nitrogen N₂ originating in the co-flowing air.

The Reynolds number for the jet, based on the inlet velocity and the inner diameter of the pipe, is approximately 16700, indicating that the jet is fully turbulent. Under these circumstances, both the mixing and the reactions processes in the jet are significantly influenced by the turbulent nature of the flow. To account for the turbulence when solving for the flow field, the $k-\omega$ turbulence model is applied.

Taking advantage of the symmetry, a two-dimensional model using a cylindrical coordinate system is solved.

3. Turbulent Reaction Rate

When using a turbulence model in a reacting flow interface, the production rate (kg/ (m³·s)) of species i resulting from reaction j is modeled as the minimum of the mean-value-closure reaction rate and the eddy-dissipation-model rate:

$$R_{ij} = \nu_{ij} M_i \cdot \min [r_{MVC,j}, r_{ED,j}] \quad (3)$$

The mean-value-closure rate is the kinetic reaction rate expressed using the mean mass fractions. This corresponds to the characteristic reaction rate for reactions which are slow compared to the turbulent mixing, or the reaction rate in regions with negligible turbulence levels. This can be quantified through the Damköhler number, which compares the turbulent time scale (τ_T) to the chemical time scale (τ_C). The mean-value-closure is appropriate for low Damköhler numbers:

$$Da = \frac{\tau_T}{\tau_C} \ll 1$$

The reaction rate defined by the eddy-dissipation model [10] is:

$$r_{ED,j} = \frac{\alpha_j}{\tau_T} \rho \cdot \min \left[\min \left(\frac{\omega_r}{\nu_{rj} M_r} \right), \beta \sum_P \left(\frac{\omega_P}{\nu_{pj} M_P} \right) \right] \quad (4)$$

where τ_T (s) is the mixing time scale of the turbulence, ρ is the mixture density (kg/m³), ω is the species mass fraction, ν denotes the stoichiometric coefficients, and M is the molar mass (kg/mol). Properties of reactants of the reaction are indicated using a subscript r , while product properties are denoted by a subscript P .

The eddy-dissipation model assumes that both the Reynolds and Damköhler numbers are sufficiently high for the reaction rate to be limited by the turbulent mixing time scale τ_T . A global reaction can then at most progress at the rate at which fresh reactants are mixed, at the molecular level, by the turbulence present. The reaction rate is also assumed to be limited by the deficient reactant; the reactant with the lowest local concentration. The model parameter β specifies that product species is required for reaction, modeling the activation energy. For gaseous non-premixed combustion the model parameters have been found to be [10]:

$$\alpha = 4, \beta = 0.5$$

In the current model the molecular reaction rate of the reactions is assumed to be infinitely fast. This is achieved in the model by prescribing unrealistically high rate constants for the reactions. This implies that the production rate is given solely by the turbulent mixing in (4).

It should be noted that the eddy-dissipation model is a robust but simple model for turbulent reactions. The reaction rate is governed by a single time scale, the turbulent mixing time-scale. For this reason, the

AEC008

reactions studied should be limited to global one step (as in (2)), or two step reactions

4. Heat of Reaction

The heat of reaction, or change in enthalpy, following each reaction is defined from the heat of formation of the products and reactants:

$$\Delta H_r = \sum_{\text{product}} \Delta H_f - \sum_{\text{reactants}} \Delta H_f \quad (5)$$

The heat of formations for each species is given in Table 1 [11]. Since the heat of formation of the products is lower than that of the reactants, both reactions are exothermic and release heat. The heat release is included in the model by adding a Heat Source feature to the Heat Transfer in Fluids user interface. The heat source (W/m³) applied is defined as:

$$q = r_{ED,1} \Delta H_{r1} + r_{ED,2} \Delta H_{r2} \quad (6)$$

Table 1 Species enthalpy of formation and heat capacity

Species	ΔH_f (cal/mol) T = 298 K	Cp (cal/(mol·K))	Cp (cal/(mol·K))	Cp (cal/(mol·K))
N2	0	6.949	7.830	8.601
H2	0	6.902	7.209	8.183
O2	0	7.010	8.350	9.032
H2O	-57.80	7.999	9.875	12.224
CO	-26.420	47.259	6.950	7.948
CO2	-94.061	51.140	8.910	12.993

5. Heat Capacity

The temperature in the jet increases significantly due to the heat release following the reactions, this is one of the defining features of combustion. For an accurate prediction of the temperature it is important to account for the temperature dependence of the species heat capacities. In the model, interpolation functions for the heat capacity at constant pressure, $c_{p,i}$ (cal/(mol·K)), for each species are defined using the values at three different temperatures given in Table 1. The heat capacity of the mixture, $c_{p,mix}$ (J/(kg·K)), is computed as a mass fraction weighted mean of the individual heat capacities:

$$c_{p,mix} = \sum_i \frac{\omega_i c_{p,i}}{M_i} \quad (7)$$

6. Radiation and Participating Media Interactions

The balance of the radiative intensity including all contributions (propagation, emission, absorption, and scattering) can now be formulated [12].

$$\Omega \cdot \nabla I(\Omega) = \kappa I_b(T) - \beta I(\Omega, s) + \frac{\sigma_s}{4\pi} \int_0^{4\pi} I(\Omega') \phi(\Omega', \Omega) \partial \Omega' \quad (8)$$

Where

$I(\Omega)$ is the radiative intensity at a given position

following the Ω direction

T is the temperature

κ, β, σ_s are absorption, extinction, and scattering coefficients, respectively

7. The Heat Transfer Model

The heat transfer in porous media interface is modeled based on the thermal equilibrium assumptions. The corresponding energy equation in terms of temperature is given by

$$(\rho c_p)_{\text{eff}} \frac{\partial T}{\partial t} + \rho c_p u \cdot \nabla T = \nabla \cdot (k_{\text{eff}} \nabla T) + Q \quad (9)$$

With the following material properties:

ρ is the fluid density.

c_p is the fluid heat capacity at constant pressure of mixture gas.

$(\rho c_p)_{\text{eff}}$ is the equivalent thermal conductivity (a scalar or a tensor if the thermal conductivities are anisotropic).

u is the fluid velocity field, either an analytic expression or a velocity field from a fluid-flow interface. u should be interpreted as the Darcy velocity, that is, the volume flow rate per unit cross-sectional area. The average linear velocity (the velocity within the pores) can be calculated as $u_L = u / \phi_f$ where ϕ_f is the fluid's volume fraction, or effective the porosity.

Q is the heat source (or sink). Add one or several heat sources as separate features.

The effective thermal conductivity of the solid-fluid system, k_{eff} , k_s is related to the conductivity of the solid and k_f to the conductive of fluid by

$$k_{\text{eff}} = \phi_s k_s + \phi_f k_f \quad (9.1)$$

The equivalent volumetric heat capacity of the solid-fluid system is calculated by

$$(\rho c_p)_{\text{eff}} = \phi_s \rho_s c_{s,s} + \phi_f \rho c_{p,mix} \quad (9.2)$$

Here ϕ_s denotes the solid material's volume fraction, which is related to the volume fraction of the fluid ϕ_f (or porosity) by

$$\phi_f + \phi_s = 1 \quad (9.3)$$

For a steady-state problem the temperature does not change with time, and the first term in the left-hand side of (9) disappears. This porous model considers silicon carbide (SiC) with porosity of 0.4. The corresponding values of thermal conductivity (k), density (ρ) and specific heat capacity (C_p) are 120

AEC008

$W/(m \cdot K)$, 3100 kg/m^3 and $750 \text{ J/(kg} \cdot \text{K)}$ respectively [13].

8. Solution Procedure

The syngas combustion model is solved using finite element method in three steps.

1 Use an initial sub-model to solve for isothermal turbulent flow in a straight pipe with the same diameter as the burner. The fully developed flow at the pipe outlet is then used as inlet condition for the burner.

2 Solve for the turbulent and reacting, but isothermal, flow in the round jet burner configuration.

3 Include the heat transfer and solve for the fully coupled reacting flow, using the previous solution as initial condition.

Using several solution steps is vital for a robust solution procedure when solving models with a high degree of coupling. This is the case for turbulent reacting flow that takes into account of heat transfer.

9. Results and discussion

The proposed model for the syngas non-premixed free flame is validated against the experimental data obtained by Barlow and his research group [2-4]. The results are shown in Figures 2-4.

In Figure 2 the jet temperature is examined and compared with the experiments. The temperature along the centerline is plotted. Model results are plotted using lines, while experimental results are indicated using symbols. The downstream positions are defined in terms of the inner diameter of the pipe ($Di = 4.58 \text{ mm}$). While Pl is a pipe length is equal to Di times 10. It is seen that the maximum temperature predicted in the model is close to that in the experiment. However in the model the temperature profile is shifted in the downstream direction.

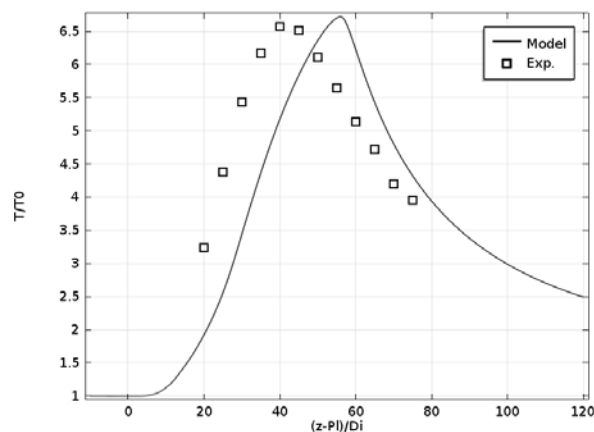


Figure 2: Jet temperature along the centerline Scaled by the inlet temperature. The centerline and radial distance is scaled by the inner diameter of the pipe.

Figure 3, using the same downstream positions. The axial velocity is found to compare well with the experimental values at both positions.

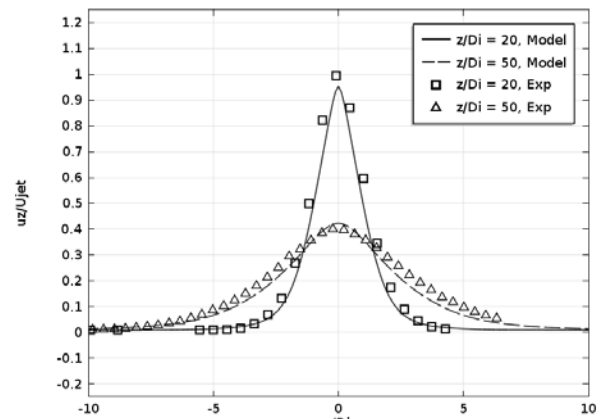


Figure 3: Axial velocity at two different positions downstream of the pipe exit, scaled by the inlet velocity. The radial distance is scaled by the inner diameter of the pipe. Model results are plotted using lines, while experimental results are indicated using symbols.

In Figure 4 the species concentration along the jet centerline is analyzed and compared with the experimental results. For fuel species, CO, and product, N_2 , the axial mass fraction development agrees well with the experimental results. The trend appears correct but the profiles are slightly difference, as is the case with the temperature. The accuracy is probably influenced by the simplified reaction scheme and the eddy-dissipation model. Nevertheless, the overall prediction of the computed data by the present mathematical model is reasonably accurate. All of the favorable comparisons lend confidence to the accuracy of the present numerical model.

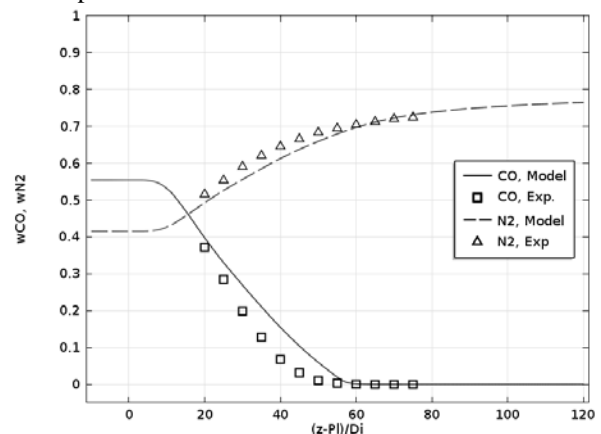


Figure 4: Species mass fractions along the jet centerline. The centerline distance is scaled

Combustion in a porous regime is then simulated. The resulting velocity field in the non-isothermal reacting jet is visualized in Figure 5. The expansion and development of the hot free jet is clearly seen. The turbulent mixing in the outer parts of the jet acts to accelerate fluid originating in the co-flow, and incorporate it in the jet. This is commonly referred to as entrainment and can be observed in the co-flow streamlines which bend towards the jet downstream of the orifice.

AEC008

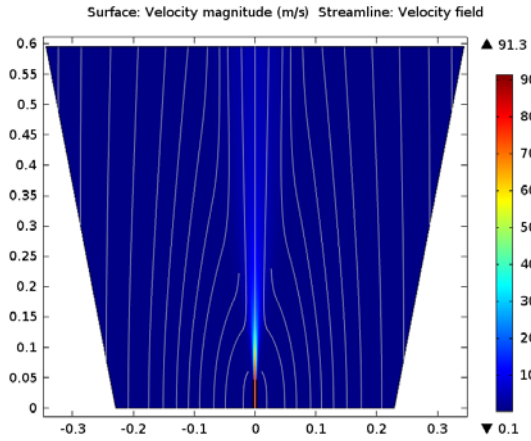


Figure 5: The velocity magnitude and flow paths (streamlines) of the reacting jet.

The temperature in the jet is shown in Figure 6 where a revolved data set has been used to emphasize the structure of the round jet. The maximum temperature in the jet is seen to be approximately 970 K.

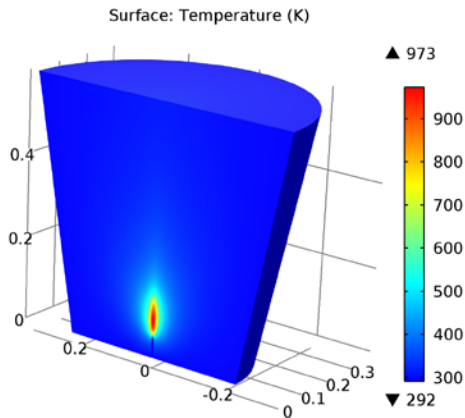


Figure 6: Jet temperature shown using a revolved data set.

The carbon dioxide mass fraction in the reacting jet is plotted in Figure 7. The formation of CO₂ takes place in the outer shear layer of the jet. This is where the fuel from the pipe encounters oxygen in the co-flow and reacts. The reactions are promoted by the turbulent mixing in the jet shear layer. It is also seen that the CO₂ formation starts just outside of the pipe. This is also the case for the temperature increase in Figure 6. This implies that there is no lift-off and the flame is attached to the pipe.

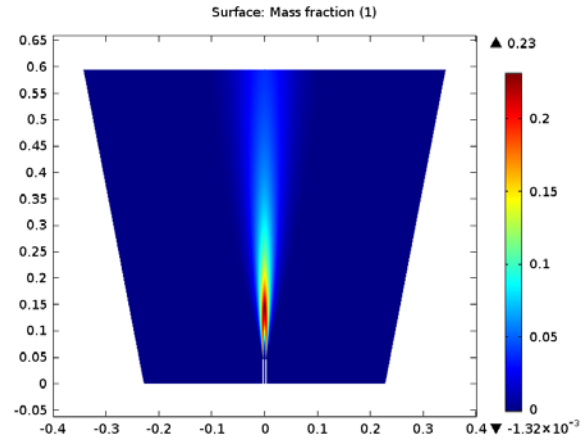


Figure 7: CO₂ mass fraction in the reacting jet.

In Figure 8 the jet temperature is further examined. In the top panel the temperature along the centerline is plotted. It is seen that the maximum temperature is about at $(z-P1)/Di = 10$. Unlike non-porous burner, the maximum temperature appears at about 55. In the bottom panel of Figure 8 temperature profiles at 20 and 50 pipe diameters downstream of the pipe exit are depicted.

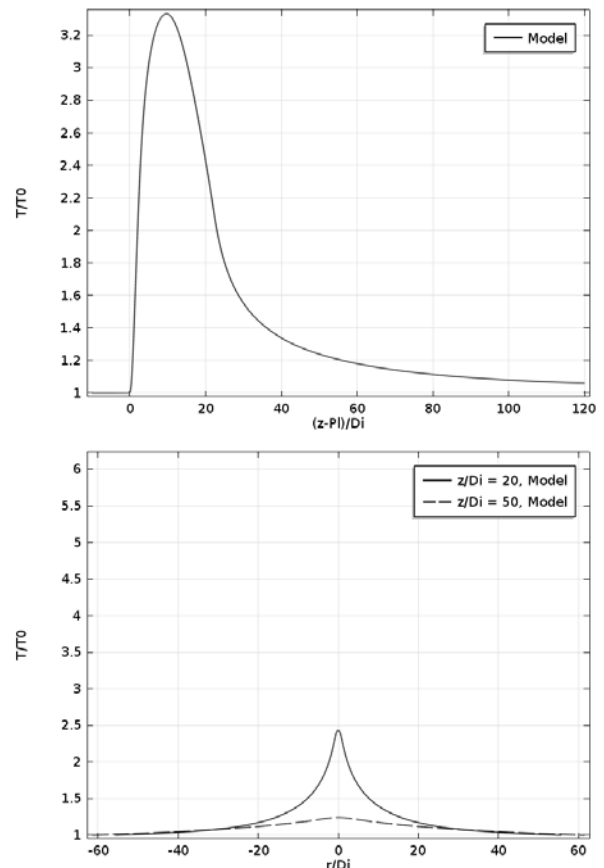


Figure 8: Jet temperature along the centerline (top), and radially at two different positions downstream of the pipe exit (under) scaled by the inlet temperature.

The centerline and radial distance is scaled by the inner diameter of the pipe. The downstream positions are defined in terms of the inner diameter of the pipe (Di).

AEC008

Figure 9, show the distributions of the axial velocity of the jet at two different positions. It can be seen that the gas velocity is faster near the pipe exit. It gets lower and more uniform away from the pipe exit.

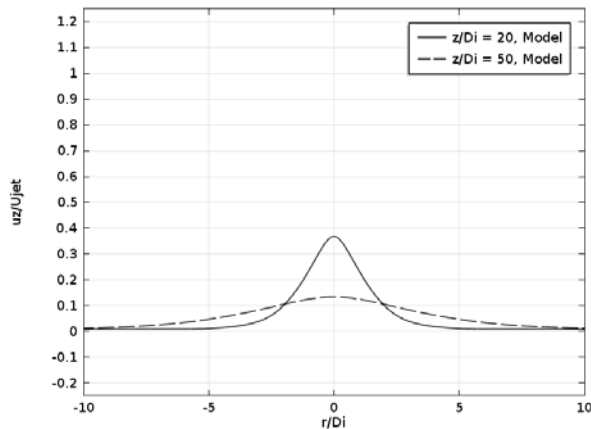


Figure 9: Axial velocity at two different positions downstream of the pipe exit, scaled by the inlet velocity. The radial distance is scaled by the inner diameter of the pipe.

In Figure 10 the species concentration along the jet centerline is analyzed. For species, CO, and N₂, the trend appears the same at case with non-porous burner in figure 7 but the profiles are slightly different, as was the case for the fuel species CO and H₂ as observed. Lately for the remaining species, O₂ and H₂O. The results show different slope between porous and non-porous burner (fig 3). It is found that reactions rate in porous burner is faster.

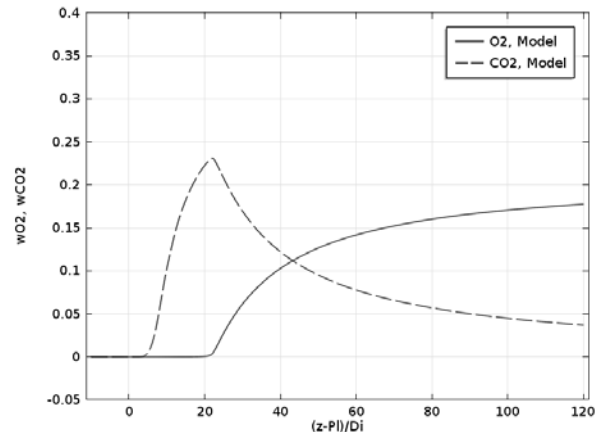
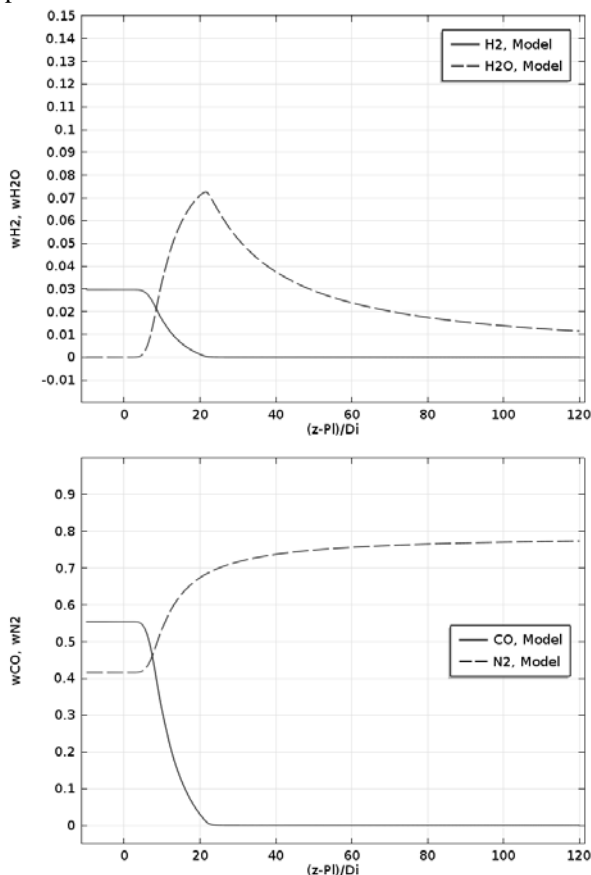


Figure 10: Species mass fractions along the jet centerline. The centerline distance is scaled

10. Conclusion

The non-premixed combustion of syngas in a round-jet porous burner is numerically analyzed. The computed results of jet temperature, axial velocity and species mass fractions are compared with the non-porous burner. The maximum temperature when using the porous burner is shifted closer to the pipe exit. The reactions rate is faster while the overall velocity is reduced. The reason of the differences between the two cases can be mainly attributed to the effect of porous solid matrix on the flame that is more stabilized.

11. References

- [1] Ranga Dinesh, K.K.J., Jiang, X., Van Oijen, J.A. (2013). Direct numerical simulation of non-premixed syngas burning with detailed chemistry, *Fuel*, vol 107, 2013, pp. 343-355.
- [2]. Cuoci, A, Frassoldati, A., Buzzi, Ferraris G., Faravelli, T., Ranzi, E. (2007). The ignition, combustion and flame structure of carbon monoxide/hydrogen mixtures. Note 2: Fluid dynamics and kinetic aspects of syngas combustion, *Int. J. Hydrogen Energy*, vol. 32(15), October 2007, pp. 3486 – 3500
- [3] Barlow, R. S., Fiechtner, G. J., Carter, C. D., Chen, J.-Y. (2000). Experiments on the Scalar Structure of Turbulent CO/H₂/N₂ Jet Flames, *Comb. and Flame*, vol. 120(4), March 2000, pp. 549-569.
- [4] Flury, M. (1998). Experimentelle Analyse der Mischungstruktur in turbulenten nicht vorgemischten Flammen, Ph.D. Thesis, ETH Zurich, 1998.
- [5] Barlow, R.S. et al., (2002). *Sandia/ETH-Zurich CO/H₂/N₂ Flame Data - Release 1.1*, URL: <http://www.ca.sandia.gov/TNF>, accessed on 04/08/2015
- [6] Tarokh, A., Mohamad, A.A., and Jiang L. (2009). Non-premixed CH₄ combustion in a porous media, paper presented in *ASME International Mechanical Engineering Congress and Exposition*, Florida, USA.

AEC008

- [7] Pickenacker, O. (1995). Diplomarbeit, Institute of Fluid Mechanics, University of Erlangen-Nuremberg.
- [8] Brenner, G., Pickenacker, K., Trimis, D., Wawrzinek, K., and Webber, T. (2000). Numerical and Experimental Investigation of Matrix-Stabilized Methane/Air Combustion in Porous Media. *Combustion and Flame*. Vol 123(1-2), October 2000, pp. 201-213.
- [9] Wawrzinek, K., Kesting, A., Kunzel, J., Pickenacker, K., Pickenacker, O., Trimis, D., Franz, M. and Hartel, G. (2001). Experimental and numerical study of applicability of porous combustors for HCl synthesis. *Catalysis Today*. Vol. 69(3-4), pp. 393-397
- [10] Magnussen, B.F. and Hjertager, B.H., (1976). On Mathematical Modeling of Turbulent Combustion with Special Emphasis on Soot Formation and Combustion, *16th Symp (Int.) on Combust*, August 1976, pp.719–729.
- [11] Frassoldati, A., Faravelli, T. and Ranzi E. (2007). The Ignition, Combustion and Flame Structure of Carbon Monoxide/Hydrogen Mixtures. Note 1: Detailed Kinetic Modeling of Syngas Combustion Also in Presence of Nitrogen Compounds, *Int. J. Hydrogen Energy*, vol. 32(15), October 2007, pp. 3471 – 3485.
- [12] Modest, M.F. (2003). Radiative heat transfer, 2nd ed., Academic Press, San Diego, California,
- [13] Accuratus Corporation, New jersey, USA (2013). *Silicon Carbide, SiC Ceramic Properties*, URL: <http://accuratus.com/silicar.html>, accessed on 05/08/2015